Coherent absorption of light by graphene and other optically conducting surfaces in realistic on-substrate configurations

S. Zanotto, F. Bianco, V. Miseikis, D. Convertino, C. Coletti, and A. Tredicucci

Citation: APL Photonics **2**, 016101 (2017); doi: 10.1063/1.4967802
View online: http://dx.doi.org/10.1063/1.4967802
View Table of Contents: http://aip.scitation.org/toc/app/2/1
Published by the American Institute of Physics

Coherent absorption of light by graphene and other optically conducting surfaces in realistic on-substrate configurations

S. Zanotto,[1,a] F. Bianco,[2,a,b] V. Miseikis,[3] D. Convertino,[3] C. Coletti,[3] and A. Tredicucci[2,4,5]

[1]*Consiglio Nazionale delle Ricerche—Istituto Nazionale di Ottica and LENS, Via Nello Carrara 1, 50019 Sesto Fiorentino, Firenze, Italy*
[2]*NEST, Istituto Nanoscienze—CNR and Scuola Normale Superiore, P.za S. Silvestro 12, 56127 Pisa, Italy*
[3]*Center for Nanotechnology Innovation @NEST, Istituto Italiano di Tecnologia, P.za S. Silvestro 12, 56127 Pisa, Italy*
[4]*Dipartimento di Fisica "E. Fermi," Università di Pisa, Largo Pontecorvo 3, 56127 Pisa, Italy*
[5]*Fondazione Bruno Kessler (FBK), via Sommarive 18, 38123 Povo, Trento, Italy*

(Received 22 March 2016; accepted 2 November 2016; published online 23 November 2016)

Analytical formulas are derived describing the coherent absorption of light from a realistic multilayer structure composed by an optically conducting surface on a supporting substrate. The model predicts two fundamental results. First, the absorption regime named coherent perfect transparency theoretically can always be reached. Second, the optical conductance of the surface can be extrapolated from absorption experimental data even when the substrate thickness is unknown. The theoretical predictions are experimentally verified by analyzing a multilayer graphene structure grown on a silicon carbide substrate. The graphene thickness estimated through the coherent absorption technique resulted in good agreement with the values obtained by two other spectroscopic techniques. Thanks to the high spatial resolution that can be reached and high sensitivity to the probed structure thickness, coherent absorption spectroscopy represents an accurate and non-destructive diagnostic method for the spatial mapping of the optical properties of two-dimensional materials and of metasurfaces on a wafer scale. [http://dx.doi.org/10.1063/1.4967802]

Optics of conducting surfaces (i.e., surfaces displaying mainly real ac conductivity at the frequencies considered) has experienced in the past decade major breakthroughs. Initially, researchers established the concept of metasurface, where subwavelength conducting elements (traditionally metals) enable to shape the incident beam in the spatial and temporal domains.[1–3] Afterwards, thanks to graphene and other two dimensional (2D) materials, which exhibit large values of the optical conductivity on a broad frequency band, remarkable non-linear optical response and tunability properties were demonstrated.[4–8] In addition, the conjunction of the two concepts above is expected to further boost the research field, thanks to the huge potential offered by 2D materials patterned as a metasurface[9–11] and by hybrid devices where a metallic metasurface is coupled to 2D conductors.[12–14]

Whether based on 2D materials, traditional metals, or innovative alloys,[15] a (structured) optically conducting surface (OCS) shows a certain degree of energy loss, due to the very nature of the conductors which constitute the device. Such losses may be either detrimental or functional, depending on the intended application. For instance, wavefront-shaping devices and nonlinear optical components would perform better in the absence of losses, while wave filters, sensors, thermal emitters,

[a]S. Zanotto and F. Bianco contributed equally to this work.
[b]Author to whom correspondence should be addressed. Electronic mail: federicabianco82@gmail.com

and memory surfaces have opposite requirements. Hence, in general, it is of paramount importance to have a precise control over the absorption of an OCS.

Due to the extremely thin nature of two-dimensional materials and/or the implementation of patterns that are geometrically disconnected, in most cases OCSs are placed on top of a substrate. If the substrate is transparent and the back surface is optically flat, the absorption of the surface can be tailored interferometrically via a second beam incident on the substrate back surface. By properly calibrating its phase and amplitude, absorption regimes otherwise not reachable in a single-beam arrangement can be achieved, such as coherent perfect absorption (CPA) and coherent perfect transparency (CPT).[16] In the present article, we will derive analytical formulas describing coherent absorption of light in a realistic sample arrangement consisting of an OCS placed on top of a transparent, optically flat substrate. From the theory, two key points stand out: first, CPT can theoretically always be achieved. Second, the measurement of the ellipse minimum in the imbalanced two-beam coherent absorption setup is able to reveal the conductance of an OCS also when the thickness of the supporting substrate is unknown. A technique for nondestructive wafer scale diagnosis of optically conducting surfaces is hence enabled. This technique has a remarkable potential for instance when considering multilayer graphene sheets, whose thickness determination is necessary for applications in optics[17–20] and electronics.[21–23] Currently, several methods are used for estimating the multilayer graphene thickness. However, some limitations and/or drawbacks characterize these methods. For example, low-energy electron microscopy (LEEM) determines the graphene number of layers from the quantized oscillations in the electron reflectivity, but its application is generally restricted to conductive substrates and its reliability is limited up to 10 layers.[24] Thickness evaluation by ordinary micro-Raman spectroscopy can be based on the determination of the changes occurring to the width, shape, position, and intensity of the 2D band for samples containing up to 10 layers,[25] on monitoring the power of the laser beam reflected from the sample in a slightly modified micro-Raman setup,[26] or on quantifying the attenuation factor of the substrate Raman signal in the presence of the graphene layers.[27] Nevertheless, the latter two micro-Raman methods cannot be applied on graphene sheets thicker than 40 monolayers. Alternatively, atomic force microscopy (AFM) is a method that can be applied in case of graphene on smooth substrates.[26] Although this technique would allow the investigation of very thick graphene, it is mainly appropriate to the case of flakes, whereas it fails for large area graphene, as the multiple layers cover the entire substrate surface. This imposes a destructive patterning of the graphene sheets to create the necessary graphene/substrate steps for the graphene thickness determination. Moreover, the surface morphology is another fundamental aspect that has to be considered when using AFM. High roughness of substrates like silicon carbide, where terraces and steps are created during the graphitization process, may prevent to distinguish graphene areas with different number of layers. Hence, although the present technique seems at par with the aforementioned traditional methods when considering only few-layer graphene characterization, it would constitute a simple tool for assessing in a non-destructive way the properties of films composed by a high number of graphene layers, furthermore overcoming substrate morphology limitations. In addition, the concept is generally applicable to all those OCSs having mostly real ac conductivity.

The physical situation under analysis is represented in Fig. 1(a). An OCS, here schematized as a graphene layer, is placed on top of a substrate having thickness L and refractive index n. The structure is excited by two coherent parallel-propagating plane wave beams of amplitudes s_1^+ and s_2^+, while s_1^- and s_2^- represent the amplitude of the output beams. The scheme in Fig. 1(b) represents the experimental setup employed to study a sample consisting of multilayer graphene grown on a silicon carbide substrate. In the following, we will provide analytical expressions concerning the CPA/CPT related quantities for the general model structure of Fig. 1(a), while the experimental results obtained through the setup schematized in Fig. 1(b) will be detailed in the second part of the article.

Analytic expressions for the (coherent) absorption properties of a substrate-supported OCS. To explore the phenomenology of CPA/CPT in substrate-supported optically conducting surfaces and to determine analytical expressions that summarize their general properties, we derive the scattering matrix (S-matrix) of the system, which encodes the full information about its linear optical response. We base the present discussion on the general formalism described in Ref. 28, calculating the specific S-matrix for the present class of devices. The S-matrix relates the incoming waves with the outcoming waves: with reference to Fig. 1(a), $(s_1^-, s_2^-)^t = S\ (s_1^+, s_2^+)^t$. The S-matrix can be calculated explicitly

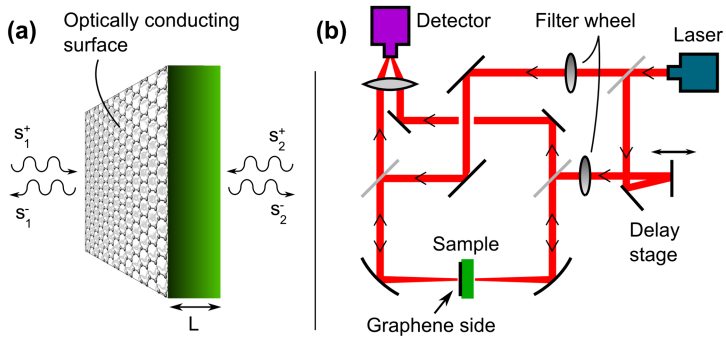

FIG. 1. (a) Schematics of the system under analysis. An optically conducting surface, here represented as a graphene sheet, lies on a transparent substrate of thickness L. Plane waves excite the system from both sides. (b) Experimental setup employed for the study of coherent modulation of absorption on a graphene sample grown on a silicon carbide substrate.

by first calculating the transfer matrix (T-matrix) of the system (by sequential multiplication of the T-matrices of the system subelements), and then converting it into the corresponding S-matrix.[29,30] Its analytical expression then reads

$$S = \frac{2}{(2+G\eta_0)\cos\varphi + i\frac{n^2+1+G\eta_0}{n}\sin\varphi}\begin{pmatrix} -G\eta_0\cos\varphi - i\frac{n^2-1+G\eta_0}{n}\sin\varphi & 2 \\ 2 & -G\eta_0\cos\varphi - i\frac{n^2-1-G\eta_0}{n}\sin\varphi \end{pmatrix}, \tag{1}$$

where G is the (possibly complex) OCS conductance, $\eta_0 = 377\ \Omega$ is the free-space wave impedance, n is the substrate refractive index, and $\varphi = 2\pi nL/\lambda_0$ is the optical path through the substrate, λ_0 being the free-space wavelength.

This analytical expression allows for some insightful observations. First, we focus the attention on the single-beam absorbance (A) by a free-standing OCS. Following from the above equation, it straightforwardly reads $A = 4\mathrm{Re}(G)\eta_0/|2 + G\eta_0|^2$. In the case here considered of an optically conducting surface, we can assume G to be approximately real (see the supplementary material for the slight modifications introduced when G becomes complex). The function $A(G)$ is monotonic in the two intervals $G\eta_0 \in (0,2)$ and $G\eta_0 \in (2,\infty)$, hence the conductance determines univocally the absorption. On one side, absorption can be tuned by a proper manipulation of the OCS conductance; on the other, the conductance can be measured relying upon an absorption measurement (provided of course one knows at least in which of the two above intervals G is expected). However, this result relies on a quite abstract arrangement, namely, that of a suspended OCS. Instead, most the practical situations involve an OCS placed on top of a transparent substrate: in this case, if the back surface of the substrate is polished, multiple reflections may occur, and the observations given so far are no more valid. The presence of multiple reflections ends up in Fabry–Pérot resonances, hence the single-beam absorption A will depend on the substrate round trip phase 2φ and it will no more be possible to extrapolate the conductance from an ordinary absorption measurement.

Significantly, it turns out that this limitation can be overcome by relying on the coherent absorption properties of the substrate-supported OCS. For clarity purposes, we recall here the general theory of coherent absorption in asymmetric two-port systems reported in Ref. 28. The joint absorbance (i.e., the quantity of incident energy absorbed by the system when it is illuminated by two coherent beams) reads

$$A_{\mathrm{joint}} = \frac{1+x}{2}A_1 + \frac{1-x}{2}A_2 - \sqrt{1-x^2}A_{\mathrm{mod}}\sin(\psi+\delta). \tag{2}$$

The joint absorbance sweeps from a minimum to a maximum, depending on the angle ψ which is the *external* dephasing, i.e., the phase difference $\arg(s_2^+/s_1^+)$ between the input beams. A_1 and A_2 are the single-beam absorbances, i.e., the absorbance observed when the system is excited by either side 1 or side 2. The joint absorbance modulation is connected to the single-beam absorbance

and the S-matrix determinant through $A_{mod} = \sqrt{(1 - A_1)(1 - A_2) - |\det S|^2}$, while δ is a characteristic phase whose actual value is not of relevance for the present discussion. Finally, x is the imbalance factor accounting for the power difference between the two-beam input intensities: $x = (|s_1^+|^2 - |s_2^+|^2)/(|s_1^+|^2 + |s_2^+|^2)$.

According to Equation (2), the joint absorbance reaches extreme values when $\sin(\psi + \delta) = \pm 1$; those extremes are elliptically dependent on the imbalance factor x, as generically depicted in Fig. 2(a). The joint absorbance can be thus described in terms of the amplitude (i.e., the ellipticity) and of the inclination angle of the ellipse. In fact, the ellipse amplitude is quantified by means of the joint absorbance modulation A_{mod}, whereas the inclination angle of the ellipse is determined by the single-beam absorbances A_1 and A_2. Other important parameters are the minimum and maximum joint absorbance, A_{min} and A_{max}. These quantify the amount of transparency (A_{min}) and of absorption enhancement (A_{max}) that can be achieved by properly modulating the amplitudes and the phases of the input beams. To connect with the notation given above, we recall that $A_{max} = 1$ means CPA, where complete absorption of the incident light occurs. Contrarily, when $A_{min} = 0$, the system is in CPT, which means that it behaves as a perfectly transparent element.

In the present model of an OCS supported by a transparent layer, all the joint absorption parameters entering Equation (2) depend on three quantities: G, n, and φ. We have performed a systematic analysis of how the joint absorption parameters depend upon G and φ, while keeping fixed n = 2.6. The latter choice is motivated by the experimental situation that will be analyzed later on, i.e., that of graphene supported by a silicon carbide slab. Again, being interested in studying the coherent absorption properties of 2D systems in which the optical response is mainly dominated by the ac conductivity, we consider first the case of a real conductance G, i.e., when the imaginary part of G assumes sufficiently small values compared to Re(G) (typically Im(G)/Re(G) $<\approx 0.1$). Notice that, at optical frequencies, graphene lies safely within that bound.[31,32] This is also true at room temperature and for quite large doping levels ($E_F \approx 300$ meV), as well as for decoupled multilayers, where the conductance scales linearly with the number of layers and the ratio Im(G)/Re(G) remains constant.[32,33]

Panels ((b)–(d)) in Fig. 2 represent the "primitive" parameters entering Equation (2), and reveal that their dependence on G and φ is entangled. The vertical axes report both the conductance in Ω^{-1} for a generic conducting surface and the corresponding number N_G of graphene monolayers, calculated assuming that the conductance of such a graphene multilayer[33] is $G = N_G G_0 = N_G \times e^2/4\hbar \approx N_G \times 6.08 \times 10^{-5}\ \Omega^{-1}$.

One remarkable feature of the present system is that CPT can theoretically *always* be obtained (see Fig. 2(a)). In CPT condition, the imbalance factor x assumes the value x_{min}; it is interesting to

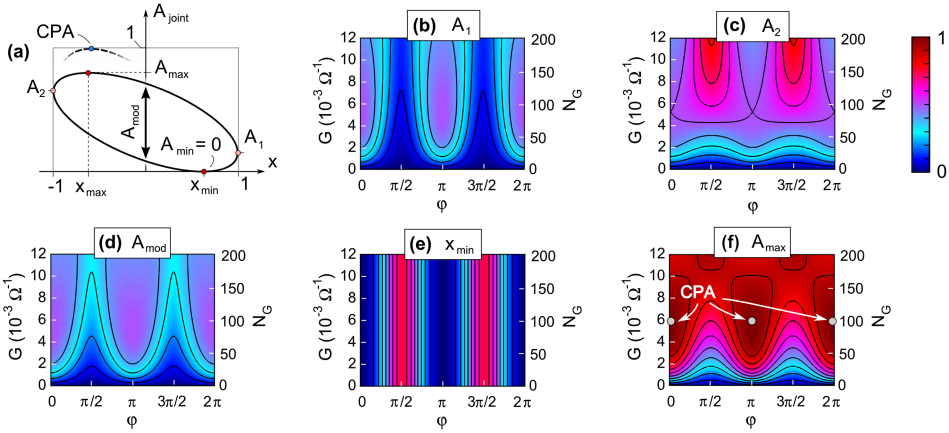

FIG. 2. Principal quantities connected to the coherent absorption from a surface of real conductivity G placed on a substrate having refractive index n = 2.6 and thickness L such that $\varphi = 2\pi nL/\lambda_0$. Summarizing scheme of the coherent absorption ellipse (panel (a)), single beam absorbances (panels (b) and (c)), absorption modulation (panel (d)), minimizing imbalance (panel (e)), and maximum joint absorption (panel (f)) are plotted. N_G indicates the number of decoupled graphene monolayers corresponding to the conductivity G.

note that x_{min} is strictly independent of G (Fig. 2(e)), and its knowledge provides then straightforward independent access to the value of φ. It is then easy to determine G directly from any of the absorption parameters. If G were not exactly real, the maximum relative error on its determined value, and hence in the numbers of layers, is of the same order of the ratio Im(G)/Re(G) (see the supplementary material for more details and for a calculation of such error as a function of Re(G) and φ for the exemplary case when Im(G)/Re(G) = 0.1 is assumed.). Note, however, that CPT and the x_{min} value are strictly independent of G, even when G is complex (see the supplementary material).

Finally, the model reveals that CPA only occurs for certain combinations of the conductance ($G \approx 6 \times 10^{-3}$ Ω^{-1}, corresponding to a graphene thickness $N_G \approx 100$) and optical phase ($\varphi = n\pi$, with n = 0, 1, 2 ...), as pointed out in Fig. 2(f). In the more general picture of a complex-valued G, the behavior of CPA is less obvious. The numeric analysis shows that CPA points may still exist, albeit for different values of Re(G) and φ. Intriguingly, CPA points eventually disappear as the ratio Im(G)/Re(G) is increased (Figs. 3(a)–3(c)). To better quantify this phenomenon we reported in Fig. 3(d) the maximum value of A_{max} which can be achieved as Re(G) and φ are varied, for a given ratio Im(G)/Re(G) and a given substrate refractive index. Notably, there exists a clear threshold of the ratio Im(G)/Re(G) above which, for a given n, CPA cannot be achieved for any combination of Re(G), Im(G), and φ. This phenomenon can be referred to as *inductively induced CPA suppression*, since it originates from the strength of the inductive response of the optically conducting surface. This result contradicts the common perception that CPA can take place independently of how small Re(G), and hence the absorption coefficient, is (a concept applicable instead to 3D systems whose thickness can be arbitrarily increased).

Coherent absorption as a probe for the properties of multilayer graphene. Inspired by the present formalism, the coherent absorption of a real two-dimensional material on substrate was experimentally studied. The system consisted in multilayer graphene grown via chemical vapor deposition (CVD) on the carbon-terminated surface of an insulating silicon carbide substrate (4H-SiC (000-1)); more details on the growth parameters are reported elsewhere.[18] The graphene is composed of 30 ± 5 electronically decoupled layers, as confirmed by the single-Lorentzian shape of the 2D peak in the Raman spectrum (Fig. 4(a)). The decoupled nature ensures that the optical properties of the sample arise from the superposition of the monolayer-like optical response of each layer. The number of layers was estimated by considering the flat graphene sheet transmittance in the mid-infrared measured by Fourier transform infrared spectrometer (not shown). The same number of layers was also evaluated

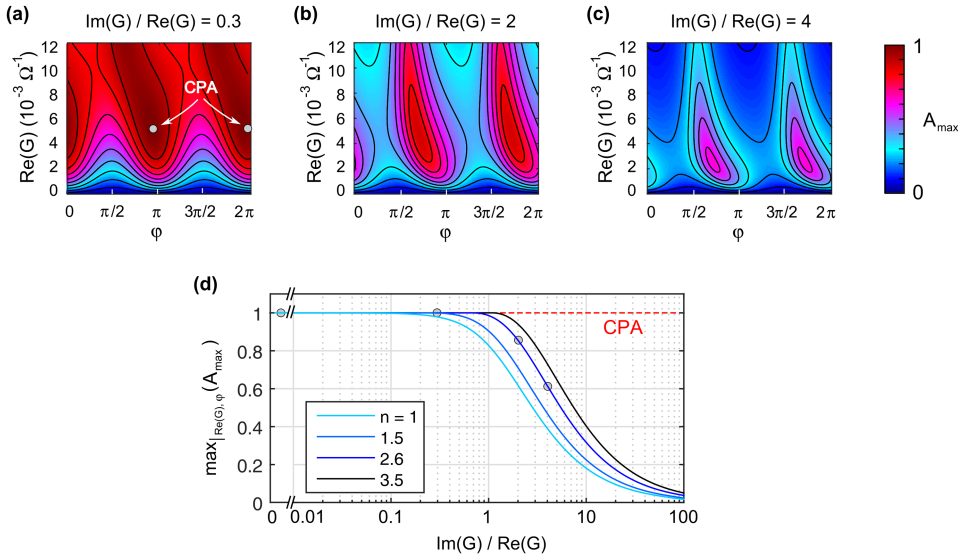

FIG. 3. Maximum joint absorption A_{max} (panels (a), (b), and (c)) from a surface of complex conductivity G, placed on a substrate having refractive index n = 2.6, calculated for three different values of the Im(G)/Re(G) ratio. (d) Maximum values of A_{max} achieved in the Re(G)-φ phase space as function of Im(G)/Re(G). Dots refer to the case of Fig. 2 (Im(G)~0) and to the three values of Im(G)/Re(G) of panels ((a)–(c)).

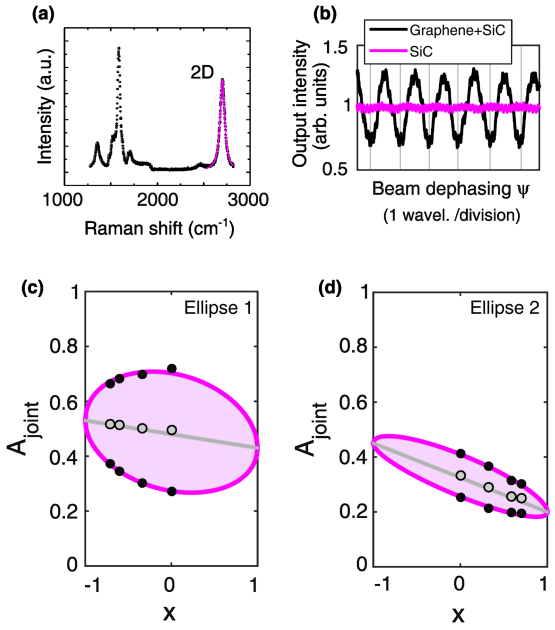

FIG. 4. (a) Representative Raman spectrum measured at 532 nm. The magenta line is the single-Lorentzian fit of the 2D peak; (b) example of measured signal under double-beam illumination of the graphene on SiC (black line) and bare SiC (magenta line) for balanced beams. The signals were normalized to their mean values for the comparison; (c) and (d) joint absorption as a function of the beam imbalance x for two different probed areas on the sample. Dotted points are the experimental data, corresponding to the maximum, minimum (black dots), and mean (grey dots) values of the A_{joint} measured for each imbalance factor x, and magenta lines are the fitting curves according to Eq. (2).

by quantifying the attenuation factor of the substrate Raman signal in the presence of graphene in the visible region.[27] In both cases, the 97.7% transmittance (2.3% absorption) was assumed per single layer.

In order to measure the coherent absorption of the system, a 633 nm He-Ne laser was split into two beams. These were then focused with a beam waist of about 30 μm onto the graphene (beam 1) and SiC (beam 2) surface, as shown in Fig. 1(b). With this setup, the spatial resolution can be tailored by selecting the proper focusing lenses. The phase delay ψ between the two beams was realized by inserting a mechanical delay stage in the optical path of beam 2. The intensity imbalance of the two beams was instead controlled by neutral filter wheels. A silicon-based detector coupled to an oscilloscope was employed to measure the intensity of the output signals when illuminating the sample with a single or double beam.

By dephasing the input beams, the absorption properties of the graphene-based system were coherently modulated. First, balanced input beams were used. As shown in Fig. 4(b), the result was a sinusoidal output intensity, whose mean value and amplitude are related to the joint absorbance and joint absorbance modulation. Remarkably, no similar behaviour was observed when investigating the bare SiC substrate (magenta line in Figure 4(b)).

Subsequently, the sample was illuminated with asymmetric beam intensities ($-1 < x < 1$ and $x \neq 0$) and the elliptical dependence on the imbalance factor x predicted by Eq. (2) was found. Figs. 4(c) and 4(d) show the experimental results for two probed areas of the sample. Notably, the two ellipses differ in amplitude and inclination angles. The difference can be understood if the theoretical model is considered. As already described, the amplitude is parametrically dependent on both graphene thickness and optical phase. Instead, the joint absorbance minimum (x_{min}) is univocally determined only by φ. Based on this consideration, we were able to estimate the φ values by extracting x_{min} from the two measured ellipses (see Table I). A φ variation of about 50% was quantified for the two areas. It is worth noting that for the sake of simplicity, the model assumed a generic φ ranging between 0 and 2π (without loss of generality). Recomputing all theoretical results by assuming the actual substrate thickness (L = 500 μm), the optical phase variation of the two areas is about 5.5%.

TABLE I. x_{min}, φ, A_{mod}, and graphene number of layers N_G estimated for the two measured ellipses. The experimental errors of x_{min} and A_{mod} are reported in brackets.

	x_{min} (±5%)	φ	A_{mod} (±5%)	N_G
Ellipse 1	0.25	0.75	0.23	28
Ellipse 2	0.78	1.57	0.10	30

This value is consistent with the 5% uncertainty of SiC thickness reported by the producer. When the optical phase is known, the model allows the graphene thickness to be quantified per each probed area. In fact, the number of layers N_G is identified by a unique combination of A_{mod} and φ values (see Fig. 2(d)). By taking into account the noise level of our present experimental setup that establishes the detectable lower bound of A_{mod}, the minimum estimable number of layers can be quantified to be as low as $N \approx 3$. From the measured joint absorbance modulations, 28 and 30 layers were estimated in area 1 and 2, respectively. These values are consistent with those obtained by FTIR and micro-Raman spectroscopy. It is worth mentioning that although different areas were investigated with the three techniques, here the graphene thickness is homogeneously distributed over the whole sample, as revealed by micro-Raman spectroscopy within various $30 \times 30\ \mu m^2$ scanned areas (lateral resolution $\approx 1\ \mu m$).

A final remark concerns coherent perfect transparency. According to the model, independently on the graphene thickness and optical phase, the minimum of the joint absorbance A_{min} is expected to be always equal to zero. However, this was not experimentally observed. Both measured ellipses exhibited $A_{min} \approx 0.2$. Taking into account the single-beam optical properties of the system and considering reliable the values of N_G and φ previously discussed, experimental reflectance and transmittance each was found to be lower than the theoretical ones by about 0.1. This discrepancy might be ascribed to two causes: first, an imperfect spatial overlap of the two incident beams could have occurred. Additionally, the incident waves might have not had a perfectly plane wavefront, contrarily to the model assumptions. Moreover, an imperfect polishing of the SiC surface might also have been responsible of further loss of detected signals. Nevertheless, the number of graphene layers estimated by means of coherent absorption agrees with that assessed by the other two spectroscopic techniques and is not influenced by these issues. The coherent absorption technique can hence be considered as a confident method for non-invasive assessment of the conductance of a sheet placed on top of a substrate, finally connected, in the case of multilayer graphene, to the number of its layers.

In conclusion, we derived analytical formulas describing the coherent absorptive properties of a realistic multilayer structure composed by a generic optical conducting surface (OCS) lying on a supporting substrate. The model pointed out that the absorption regime known as coherent perfect transparency can theoretically always be reached, independently of the sample parameters, and that the optical conductance of the OCS can be derived even when the substrate thickness is unknown. The particular case consisting of multilayered graphene sheets on a silicon carbide substrate was also analyzed. The single- and double-beam absorbances were numerically evaluated as a function of the graphene number of layers and of the substrate thickness, indicating the requisites to reach the CPA regime. To support the model, experiments of coherent absorption were performed on multilayer graphene grown on silicon carbide substrate. From the analysis of the measured ellipses, we were able to quantify the number of layers of the graphene sheet. The layer number resulted to be in good agreement with the value obtained by means of two other different techniques. The present results pave the way for a new method of characterizing the optical conductance of graphene and, more in general, of nearly 2D systems with mostly imaginary ac dielectric constant. Thanks to the potentially high lateral resolution, coherent-absorption spectroscopy represents a non-destructive diagnostic tool for the surface mapping of two-dimensional materials and of metasurfaces on a wafer scale.

See the supplementary material for the influence on the coherent absorption due to an imaginary part of the conductivity G of the optical conducting surface.

The work was partially supported by PRA_2015_0080 of Università di Pisa and by the European Union Seventh Framework Programme under Grant Agreement No. 604391 Graphene Flagship. Support from Lorenzo Pattelli and Giacomo Mazzamuto about symbolic mathematic solvers is kindly acknowledged.

[1] N. Yu and F. Capasso, Nat. Mater. **13**, 139 (2014).
[2] S. Jahani and Z. Jacob, Nat. Nanotechnol. **11**, 23 (2016).
[3] A. D. Boardman, V. V. Grimalsky, Y. S. Kivshar, S. V. Koshevaya, M. Lapine, N. M. Litchinitser, V. N. Malnev, M. Noginov, Y. G. Rapoport, and V. M. Shalaev, Laser Photonics Rev. **5**, 287 (2011).
[4] F. Parhizgar, A. G. Moghaddam, and R. Asgari, Phys. Rev. B **92**, 045429 (2015).
[5] H. Rostami and R. Asgari, Phys. Rev. B **89**, 115413 (2014).
[6] Y. Jiang, L. Miao, G. Jiang, Y. Chen, X. Qi, X. Jiang, H. Zhang, and S. Wen, Sci. Rep. **5**, 16372 (2015).
[7] S. Z. Butler, S. M. Hollen, L. Cao, Y. Cui, J. A. Gupta, H. R. Gutierrez, T. F. Heinz, S. S. Hong, J. Huang, A. F. Ismach, E. Johnston-Halperin, M. Kuno, V. V. Plashnitsa, R. D. Robinson, R. S. Ruoff, S. Salahuddin, J. Shan, L. Shi, M. G. Spencer, M. Terrones, W. Windl, J. E. Goldberger, H. R. Gutiérrez, T. F. Heinz, S. S. Hong, J. Huang, A. F. Ismach, E. Johnston-Halperin, M. Kuno, V. V. Plashnitsa, R. D. Robinson, R. S. Ruoff, S. Salahuddin, J. Shan, L. Shi, M. G. Spencer, M. Terrones, W. Windl, and J. E. Goldberger, ACS Nano **7**, 2898 (2013).
[8] F. Xia, H. Wang, D. Xiao, M. Dubey, and A. Ramasubramaniam, Nat. Photonics **8**, 899 (2014).
[9] A. Andryieuski and A. V. Lavrinenko, Opt. Express **21**, 9144 (2013).
[10] B. Vasic and R. Gajic, Appl. Phys. Lett. **103**, 261111 (2013).
[11] A. Fallahi and J. Perruisseau-Carrier, Phys. Rev. B **86**, 195408 (2012).
[12] S.-F. Shi, B. Zeng, X. Hong, H. S. Jung, A. Zettl, M. F. Crommie, and F. Wang, Nano Lett. **15**, 372 (2014).
[13] P. Q. Liu, I. J. Luxmoore, S. A. Mikhailov, N. A. Savostianova, F. Valmorra, J. Faist, and G. R. Nash, Nat. Commun. **6**, 8969 (2015).
[14] S. Zanotto, C. Lange, T. Maag, A. Pitanti, V. Miseikis, C. Coletti, R. Degl'innocenti, L. Baldacci, R. Huber, and A. Tredicucci, Appl. Phys. Lett. **107**, 121104 (2015).
[15] W. Li, U. Guler, N. Kinsey, G. V. Naik, A. Boltasseva, J. Guan, V. M. Shalaev, and A. V. Kildishev, Adv. Mater. **26**, 7959 (2014).
[16] Y. D. Chong, L. Ge, H. Cao, and A. D. Stone, Phys. Rev. Lett. **105**, 053901 (2010).
[17] I. Crassee, J. Levallois, A. L. Walter, M. Ostler, A. Bostwick, E. Rotenberg, T. Seyller, D. van der Marel, and A. B. Kuzmenko, Nat. Phys. **7**, 48 (2010).
[18] F. Bianco, V. Miseikis, D. Convertino, J.-H. Xu, F. Castellano, H. E. Beere, D. A. Ritchie, M. S. Vitiello, A. Tredicucci, and C. Coletti, Opt. Express **23**, 11632 (2015).
[19] J. Ma, H. Xuan, H. L. Ho, W. Jin, Y. Yang, and S. Fan, IEEE Photonics Technol. Lett. **25**, 932 (2013).
[20] J. Maysonnave, S. Huppert, F. Wang, S. Maero, C. Berger, W. De Heer, T. B. Norris, L. A. De Vaulchier, S. Dhillon, J. Tignon, R. Ferreira, and J. Mangeney, Nano Lett. **14**, 5797 (2014).
[21] Y. Ji, S. Lee, B. Cho, S. Song, and T. Lee, ACS Nano **5**, 5995 (2011).
[22] Y. Y. Choi, S. J. Kang, H. K. Kim, W. M. Choi, and S. I. Na, Sol. Energy Mater. Sol. Cells **96**, 281 (2012).
[23] K. M. F. Shahil and A. A. Balandin, Solid State Commun. **152**, 1331 (2012).
[24] H. Hibino, H. Kageshima, F. Maeda, M. Nagase, Y. Kobayashi, and H. Yamaguchi, Phys. Rev. B **77**, 1 (2008).
[25] A. C. Ferrari, Solid State Commun. **143**, 47 (2007).
[26] I. G. Ivanov, J. U. Hassan, T. Iakimov, A. A. Zakharov, R. Yakimova, and E. Janzén, Carbon **77**, 492 (2014).
[27] S. Shivaraman, M. V. S. Chandrashekhar, J. J. Boeckl, and M. G. Spencer, J. Electron. Mater. **38**, 725 (2009).
[28] L. Baldacci, S. Zanotto, G. Biasiol, L. Sorba, and A. Tredicucci, Opt. Express **23**, 9202 (2015).
[29] D. Pozar, *Microwave Engineering* (Wiley, 2005).
[30] B. E. A. Saleh and M. C. Teich, *Fundamentals of Photonics, 2nd Edition* (Wiley, 2007).
[31] Z. Q. Li, E. A. Henriksen, Z. Jiang, Z. Hao, M. C. Martin, P. Kim, H. L. Stormer, and D. N. Basov, Nat. Phys. **4**, 532 (2008).
[32] S. A. Mikhailov and K. Ziegler, Phys. Rev. Lett. **99**, 016803 (2007).
[33] H. Min and A. H. MacDonald, Phys. Rev. Lett. **103**, 067402 (2009).